/N-39

/7/0

β 2²

The Method of Lines in Analyzing
Solids Containing Cracks

John P. Gyekenyesi
Lewis Research Center
Cleveland, Ohio

NASA
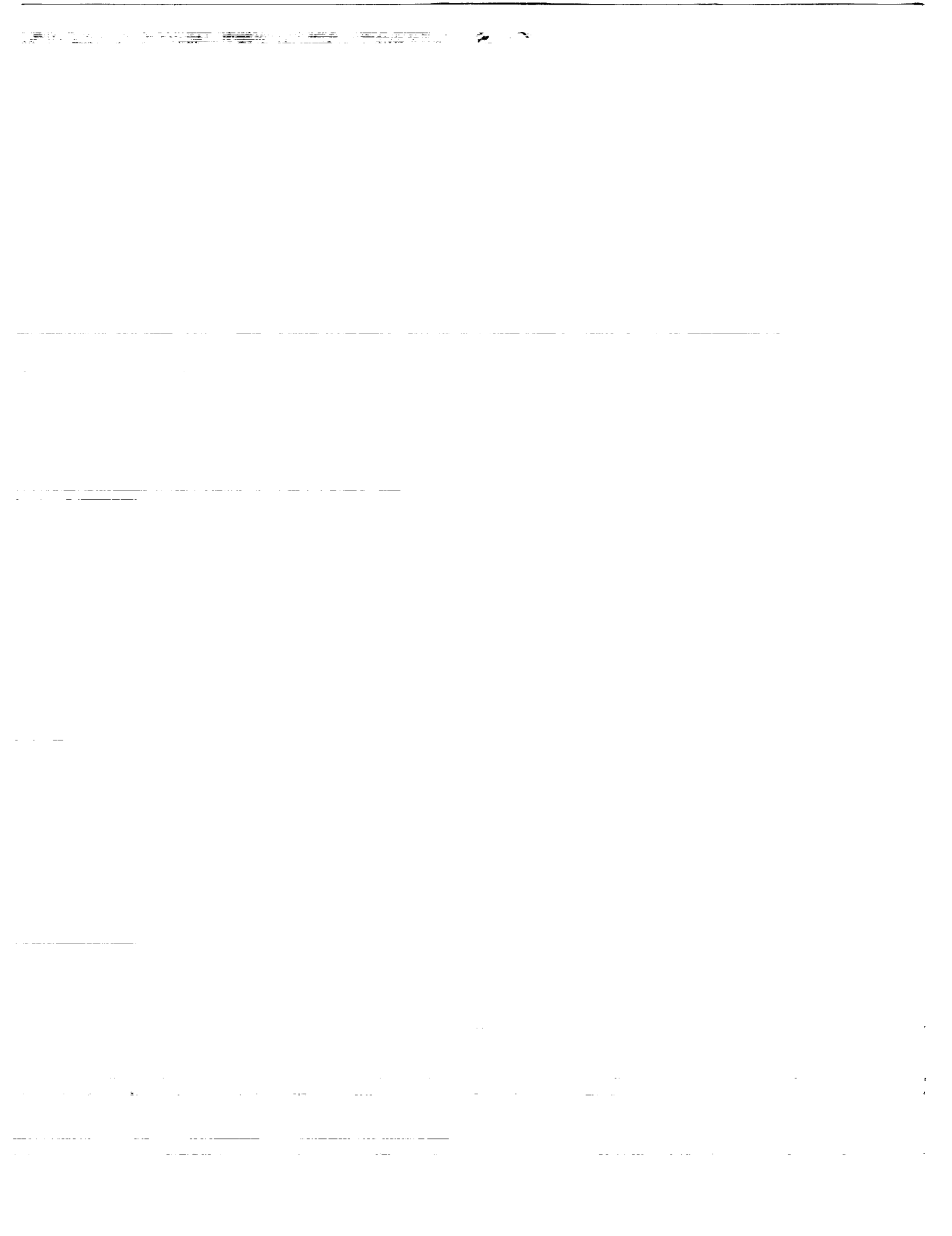
THE METHOD OF LINES IN ANALYZING SOLIDS CONTAINING CRACKS

John P. Gyekenyesi
National Aeronautics and Space Administration
Lewis Research Center
Cleveland, Ohio, U.S.A.

SUMMARY

A semi-numerical method is reviewed for solving a set of coupled partial differential equations subject to mixed and possibly coupled boundary conditions. The line method of analysis is applied to the Navier-Cauchy equations of elastic and elasto-plastic equilibrium to calculate the displacement distributions in various, simple geometry bodies containing cracks. The application of this method to the appropriate field equations leads to coupled sets of simultaneous ordinary differential equations whose solutions are obtained along sets of lines in a discretized region. When decoupling of the equations and their boundary conditions is not possible, the use of a successive approximation procedure permits the analytical solution of the resulting ordinary differential equations.

The use of this method is illustrated by reviewing and presenting selected solutions of mixed boundary value problems in three-dimensional fracture mechanics. These solutions are of great importance in fracture toughness testing, where accurate stress and displacement distributions are required for the calculation of certain fracture parameters. Computations obtained for typical flawed specimens include that for elastic as well as elasto-plastic response. Problems in both Cartesian and cylindrical coordinate systems are included. Results are summarized for a finite geometry rectangular bar with a central through-the-thickness or rectangular surface crack under remote uniaxial tension. In addition, stress and displacement distributions are reviewed for finite circular bars with embedded penny-shaped cracks, and rods with external annular or ring cracks under opening mode tension.

The results obtained show that the method of lines presents a systematic approach to the solution of some three-dimensional mechanics problems with arbitrary boundary conditions. The advantage of this method over other numerical solutions is that good results are obtained even from the use of a relatively coarse grid.

INTRODUCTION

The main goal of fracture mechanics is the prediction of the load at which a structure weakened by a crack will fail. Knowledge of the stress and displacement fields near the crack tip is of fundamental importance in evaluating this load at failure. Because of the geometric singularity associated with any crack type problem, there is almost no possibility of a simple closed form type of solution. For this reason, three-dimensional elastic solutions have been obtained only for a restricted class of problems. Furthermore, the calculation of stress and strain distributions in elasto-plastic/work hardening materials containing inherent crack-like flaws is a nonlinear and three-dimensional problem. Due to the finite boundary effect and the nonlinearity

of the material response, solutions in existence are obtained almost exclusively through numerical computer methods of continuum mechanics. Notable among these are the finite element method (refs. 1 and 2), the finite difference method (ref. 3), and the boundary integral equation method (ref. 4). These methods are useful in solving either elastic or elasto-plastic fracture mechanics problems; it is known, however that practical problems usually require a very large amount of data storage and computation time.

An alternate semi-analytical method suitable for the solution of crack problems is the line method of analysis. Successful application of this method to finite geometry solids containing cracks has been demonstrated recently for both elastic (ref. 5) and elasto-plastic (ref. 6) problems. Although the concept of the line method for solving partial differential equations is not new (refs. 7 and 8), its application in structural analysis has been limited to simple examples (ref. 9). By far the most common approach to fracture problems has been the finite element method, and it is the purpose of this paper to review a simple systematic, alternate method, the method of lines (MOL) for these problems.

The line method lies midway between completely analytical and discretized numerical methods. The basis of this technique is the substitution of finite differences for the derivatives with respect to all the independent variables except one for which the derivatives are retained. This approach replaces a given partial differential equation with a system of ordinary differential equations whose solutions can then be obtained, at least in some cases, by analytic methods. These equations describe the dependent variable along lines which are parallel to the coordinate in whose direction the derivatives were retained. Application of the line method is most useful when the resulting ordinary differential equations are linear and have constant coefficients (ref. 10).

An inherent advantage of the line method over other numerical methods is that good results are obtained from the use of relatively coarse grids. This use of a coarse grid is permissible because parts of the solutions are obtained in terms of continuous functions. It is known that MOL methods tend to keep the advantages and discard the disadvantages of both the analytical and grid methods, thereby leading to accurate solutions with minimum computation times. Another advantage of this technique is that the displacements and the normal stress and strain fields are obtained with the same degree of accuracy at each node point. The disadvantage of MOL, on the other hand, is that it tends to become numerically unstable as the number of dividing lines increases and the finite difference strip size becomes too small (refs. 8, 11 and 12). To realize a very fine space discretization with this method would require word length with much larger number of bits, leading to excessive requirements on computer resources. Current research emphasis in MOL solution methods is to overcome this problem in engineering applications (ref. 13).

GOVERNING EQUATIONS AND MOL FORMULATION

It is assumed, for simplicity of this presentation, that the material is homogeneous, isotropic and that the deformations are quasi-static and small. The structure is assumed to be elastic first and the elastic solution is taken to be known before the incipient loading is applied. As loading gradually increases, the structure becomes elasto-plastic and the governing equations are

2

written in terms of displacement increments. Using the standard summation convention, the Navier equations for the elastic problem in terms of displacements, u_i are

$$u_{i,jj} + \left(\frac{1}{1-2\nu}\right)u_{j,ji} = 0 \qquad i,j = 1,2,3 \tag{1}$$

and for the elasto-plastic regime, the displacement increments, du_i, can be obtained from

$$du_{i,jj} + \left(\frac{1}{1-2\nu}\right)du_{j,ji} = \left(\frac{1}{1-2\nu}\right)\left(\frac{d\varepsilon_p}{\sigma_e}\right)Eu_{j,ji} + 3S_{ij}\left(\frac{d\varepsilon_p}{\sigma_e}\right)_{,j} \tag{2}$$

where the body forces are assumed to be zero, $d\varepsilon_p$ is the effective plastic strain increment, S_{ij} is the stress deviator tensor and σ_e is the equivalent stress. In the plastic region the von Mises yield condition and the associated Prandl-Reuss flow rule is taken to prevail. The incremental stress-strain relations are obtained as (ref. 6),

$$\frac{d\sigma_{ij}}{2G} = d\varepsilon_{ij} + \left(\frac{\nu}{1-2\nu}\right)d\varepsilon_{kk}\delta_{ij} + \frac{3}{2}\left(\frac{d\varepsilon_p}{\sigma_e}\right)\left[\frac{E}{3(1-2\nu)}\right]\varepsilon_{kk}\delta_{ij} - \frac{3}{2}\left(\frac{d\varepsilon_p}{\sigma_e}\right)\sigma_{ij} \tag{3}$$

where ν, G, E are the conventional elastic properties, σ_{ij} is the Kronecker delta and σ_{ij} are the stresses.

In order to solve equations (1) or (2), we apply MOL and reduce these equations to systems of simultaneous ordinary differential equations. For problems in Cartesian coordinates, equations (1) can be written as

$$\nabla^2 u + \left(\frac{1}{1-2\nu}\right)\left(\frac{\partial e}{\partial x}\right) = 0 \tag{4}$$

$$\nabla^2 v + \left(\frac{1}{1-2\nu}\right)\left(\frac{\partial e}{\partial y}\right) = 0 \tag{5}$$

$$\nabla^2 w + \left(\frac{1}{1-2\nu}\right)\left(\frac{\partial e}{\partial z}\right) = 0 \tag{6}$$

where the dilatation is

$$e = \frac{\partial u}{\partial x} + \frac{\partial v}{\partial y} + \frac{\partial w}{\partial z} \tag{7}$$

and u, v, and w are the x-directional, y-directional and z-directional displacements, respectively. For a finite geometry solid with rectangular boundaries, we construct three sets of parallel lines (fig. 1(a)). Each set of lines is parallel to one of the coordinate axes and thus perpendicular to the corresponding coordinate plane. An approximate solution of equation (4) can then be obtained by developing solutions of ordinary differential equations along the x-directional lines. As seen in the figure, there are a total of $\ell = NY \times NZ$ such lines where NY is the number of lines along the y-direction and NZ is the number of lines along the z-direction in a given plane, respectively. We define the displacements along these lines as $u_1, u_2, \ldots$,

3
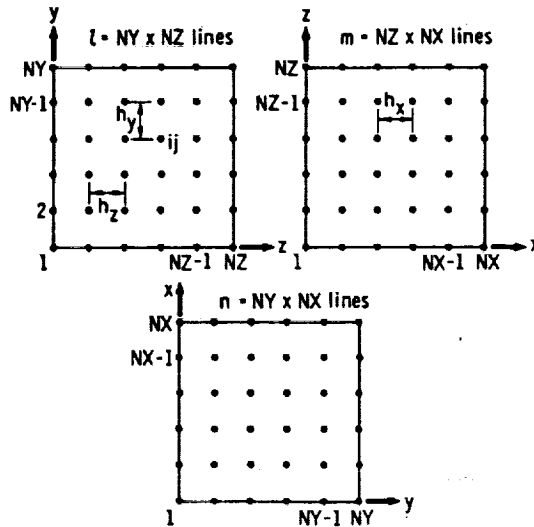
(a) Three sets of lines parallel to x-, y- and z-coordinates
and perpendicular to corresponding coordinate planes.
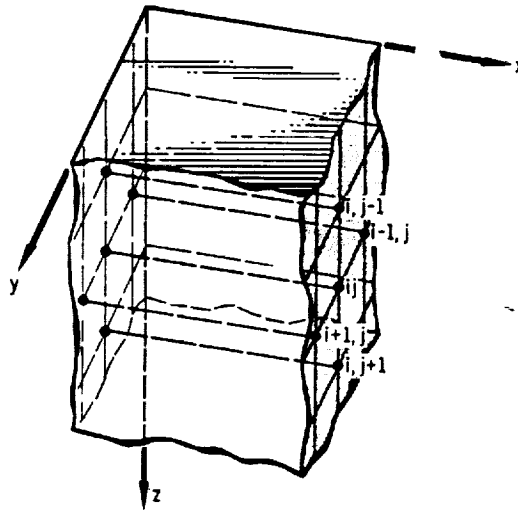
(b) Set of interior lines parallel to x-coordinate.

FIGURE 1. - SETS OF LINES PARALLEL TO CARTESIAN COORDINATES.

u_ℓ. The derivatives of the y-directional displacements on these lines with respect to y are defined as $v'|_1, v'|_2, \ldots, v'|_\ell$, and the derivatives of the z-directional displacements with respect to z are defined as $w'|_1, w'|_2, \ldots, w'|_\ell$. These displacements and derivatives can then be regarded as functions of x only since they are variables on x-directional lines. When these definitions are used the ordinary differential equation along a generic line ij (a double subscript is used here for simplicity of writing and the subscripts obviously are not related to those in the previous equations) in figure 1, using central differences with truncation errors of $O(h^2)$, may be written as

4

$$\frac{d^2u_{ij}}{dx^2} + \frac{(1 - 2\nu)}{2(1 - \nu)}\left[-\left(\frac{2}{h_y^2} + \frac{2}{h_z^2}\right) + \frac{1}{h_y^2}\left(u_{i+1,j} - u_{i-1,j}\right) \right.$$

$$\left. + \frac{1}{h_z^2}\left(u_{i,j+1} - u_{i,j-1}\right) \right] + \frac{f_{ij}(x)}{2(1 - \nu)} = 0 \qquad (8)$$

where

$$f_{ij}(x) = \frac{dv'}{dx}\bigg|_{ij} + \frac{dw'}{dx}\bigg|_{ij} \qquad (9)$$

and

$$v' = \frac{dv}{dy}; \quad w' = \frac{dw}{dz}$$

Similar differential equations are obtained along the other x-directional lines. The set of ℓ second order differential equations represented by equation (8) can be reduced to a set of 2ℓ first order differential equations by treating derivatives of the u's as an additional set of ℓ unknowns. The resulting equations can now be written as a single first order matrix differential equation

$$\frac{dU}{dx} = A_1U + R(x) \qquad (10)$$

where U and R are column matrices of 2ℓ elements each and A_1 is 2ℓ x 2ℓ matrix of coefficients. In a similar manner to solve the other two Navier equations for the elastic problem, we construct ordinary differential equations along the y- and z-directional lines, respectively. These equations are also expressed in an analogous form to equation (10); they are

$$\frac{dV}{dy} = A_2V + S(y) \qquad (11)$$

$$\frac{dW}{dz} = A_3W + T(z) \qquad (12)$$

Equations (10) to (12) are linear, first-order, ordinary differential equations. They are, however, not independent, but are coupled through the vectors R, S and T.

Noting that a second order ordinary differential equation can satisfy only a total of two boundary conditions and since three-dimensional elasticity problems have three conditions at every point of the bounding surface, the shear stress boundary data must be incorporated into the differential equations of the surface lines. The applications of the specified shear conditions permits the use of a single layer of boundary image lines when surface line differential equations are constructed.

For an elasto-plastic solid the governing differential equations for displacement increments and the incremental stress-displacement relations are found in reference 6. The x-directional displacement increments, in an analogous manner to equation (10), can be obtained from

$$\frac{d}{dx}(dU) = A_1 dU + d\bar{R}(x) \tag{13}$$

where the coupling vector $d\bar{R}(x)$ contains mixed derivative terms for elastic and plastic regions in addition to terms involving the ratio of $d\epsilon_p/\sigma_e$.

The system of ordinary differential equation (10) can be solved by any of a number of standard techniques. The method employed in references 5, 6, and 9 is the Peano-Baker method of integration. The solution can be written as

$$U(x) = e^{A_1 x} U(0) + e^{A_1 x} \int_0^x e^{-A_1 \eta} R(\eta) d\eta \tag{14}$$

where $U(0)$ is the initial value vector determined from the boundary conditions and the matrizant $e^{A_1 x}$ is generally evaluated by its matrix series. For larger values of x, when convergence becomes slow, additive formulas may be used. In addition, similarity transformations can be used to diagonalize the coefficient matrix A_1. It should be noted that, in general, the matrix A_1 is a function of Poisson's ratio and the coordinate finite difference increments. Uniform line spacing in the three coordinate directions makes closed form diagonalization of A_1 possible. However, refinement of the mesh with uniform line spacing rapidly increases the required computer time and storage as well as raises the probability of numerical difficulties in the matrix exponential power series computations. Consequently, variable mesh spacing is recommended as one method of obtaining improved answers without an increase in problem size.

Most of the previously obtained MOL solutions in fracture mechanics involved the use of finite difference formulas with truncation errors of $O(h^2)$. Recent work by Mendelson and Alam (ref. 13), uses higher order finite difference approximations as an alternate method of obtaining more accurate results. These five point finite difference approximations for the first and second y-derivatives of a function $f(x,y,z)$ at (x,y,z) can be written as (ref. 8):

$$\left(\frac{\partial f}{\partial y}\right)_{x,y,z} = \frac{4}{3}\left[\frac{f(x,y+h_y,z) - f(x,y-h_y,z)}{2h_y}\right]$$

$$-\frac{1}{3}\left[\frac{f(x,y+2h_y,z) - f(x,y-2h_y,z)}{4h_y}\right] + O\left(h_y^4\right)$$

$$\left(\frac{\partial^2 f}{\partial y^2}\right)_{x,y,z} = \frac{4}{3}\left[\frac{f(x,y+h_y,z) + f(x,y-h_y,z) - 2f(x,y,z)}{h_y^2}\right]$$

$$-\frac{1}{3}\left[\frac{f(x,y+2h_y,z) + f(x,y-2h_y,z) - 2f(x,y,z)}{4h_y^2}\right] + O\left(h_y^4\right) \tag{15}$$

Since the evaluation of the matrix exponential power series becomes increasingly difficult with the coefficients obtained through the use of equations (15), a recurrence relations method is used to solve the resulting systems of ordinary differential equations. An error analysis in reference 8 indicates that approximately six times as many dividing lines must be used with $O(h^2)$ approximations to get equivalent accuracy to that obtained when equations (15) are used.

The solution of equation (10) by recurrence relations can be obtained by taking N equal intervals along the x-axis, each having a length of h_m. Then by using finite differences for $(dU/dx)_m$ and average values of $(A_1U + R)_m$, the following linear recurrence formula will be obtained (ref. 13), expressing U_m in terms of U_{m-1}:

$$U_m = L_m U_{m-1} + M_m \tag{16}$$

where L_m is a known function of h_m and A_1 while M_m will depend on R in addition to h_m and A_1. We can also express U_m in terms of U_1 by repeated application of equation (16), leading to

$$U_m = D_m U_1 + F_m \tag{17}$$

where D_m and F_m are known functions of L_m and M_m. By suitable partitioning of D and F matrices at the boundaries, we can use given boundary data at the last station, U_n, to calculate unknown elements of U_1, where $n = N + 1$. The advantage of using equation (17) to calculate U_m, $m = 1,2,.\ .\ .,n$, is that the coefficient matrix A_1 has no limitation on its format or on the arrangement of its elements. The interval h_m can be decreased to any fraction of h_x, the initially established finite difference increment obtained from the application of MOL. Results of test problems indicate that two or three subintervals are adequate for the solution of a typical problem.

In a similar manner, for problems in cylindrical coordinates, equations (1) can be written as

$$(\partial e/\partial r) + (1 - 2\nu)[(\nabla^2 - r^{-2})u - 2r^{-2}(\partial v/\partial \theta)] = 0 \qquad (18)$$

$$r^{-1}(\partial e/\partial \theta) + (1 - 2\nu)[(\nabla^2 - r^{-2})v + 2r^{-2}(\partial u/\partial \theta)] = 0 \qquad (19)$$

$$(\partial e/\partial z) + (1 - 2\nu)\nabla^2 w = 0 \qquad (20)$$

where the dilatation is

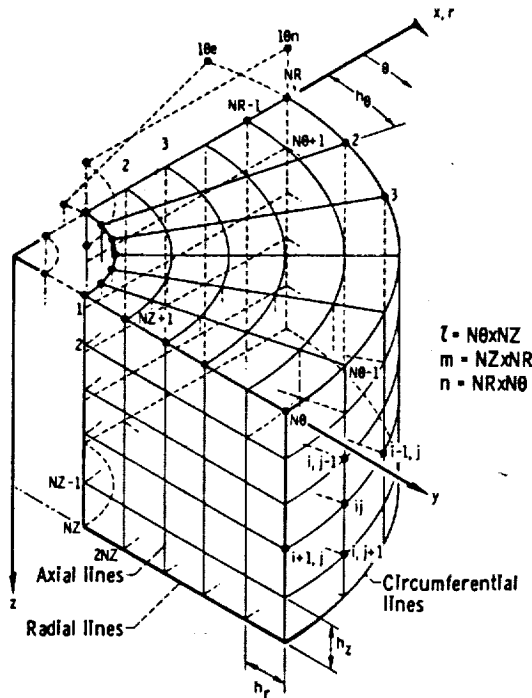$$e = (\partial u/\partial r) + r^{-1}(\partial v/\partial \theta) + (u/r) + (\partial w/\partial z).$$

FIGURE 2. - SETS OF LINES IN DIRECTION OF CYLINDRICAL COORDINATES.

For a finite geometry body with circular boundaries, we construct three sets of parallel lines in the direction of the coordinates as shown in figure 2. Approximate solutions of the above equations can then be obtained by developing solutions of ordinary differential equations along the radial, circumferential, and axial lines, respectively. For equation (18), we define the displacements along the radial lines as $u_1, u_2, \ldots, u_\ell$. The derivatives of the circumferential displacements on these lines with respect to θ are defined as $v'|_1, v'|_2, \ldots, v'|_\ell$, and the derivatives of the axial displacements with respect to z are defined as $w'|_1, w'|_2, \ldots, w'|_\ell$. These displacements and derivatives can then be regarded as functions of the radius only, since they are variables on radial lines. If these definitions are used, the ordinary differential equation along a generic, radial line ij of figure 2 may be written as

$$\left[\frac{d^2 u_{ij}}{dr^2} + \frac{1}{r}\frac{du_{ij}}{dr} - \frac{u_{ij}}{r^2}\right] + \frac{(1 - 2\nu)}{2(1 - \nu)}\left[-\left(\frac{2}{r^2 h_\theta^2} + \frac{2}{h_z^2}\right)u_{ij} + \frac{1}{r^2 h_\theta^2}(u_{i+1,j} + u_{i-1,j})\right.$$

$$\left. + \frac{1}{h_z^2}(u_{i,j+1} + u_{i,j-1})\right] + \frac{f_{ij}(r)}{2(1 - \nu)} = 0 \qquad (21)$$

where

$$f_{ij}(r) = \left[(4\nu - 3)/r^2\right]v'\big|_{ij} + r^{-1}(dv'/dr)\big|_{ij} + (dw'/dr)\big|_{ij} \qquad (22)$$

and

$$v' = dv/d\theta$$

$$w' = dw/dz$$

Similar differential equations are obtained along the other radial lines. Since each equation has the terms of the displacements on the surrounding lines, these equations constitute a system of ordinary differential equations for the displacements $u_1, u_2, \ldots, u_\ell$.

Noting that a second-order differential equation can satisfy only a total of two boundary conditions, the shear stress boundary data must again be incorporated into the surface line differential equations. For the first radial line of figure 2, the use of zero shear stress boundary conditions in the radial direction on the r,z and r,θ coordinate planes gives, respectively, the following imaginary radial line displacements:

$$u_{1\theta e} = u_2 + 2h_\theta r(dv/dr)\big|_1 - 2h_\theta v\big|_1$$

$$u_{1\theta n} = u_{N\theta+1} + 2h_z(dw/dr)\big|_1 \qquad (23)$$

Equations (23) must then be used in the application of central difference approximations when the ordinary differential equation for the first radial line is generated. Additional details on the construction of these equations can be found in reference 13.

As before the system of ℓ second order equations given by equation (21) can be written as a single first order matrix equation

$$dU/dr = A_r(r)U + R(r) \qquad (24)$$

where in this case the elements of U are defined by

$$U_1 = ru_1, \qquad U_2 = ru_2, \ldots, \qquad U_\ell = ru_\ell$$

$$(25)$$

$$U_{\ell+1} = r^{-1}[d(ru_\ell)/dr], \qquad U_{\ell+2} = r^{-1}[d(ru_2)/dr], \ldots, \qquad U_{2\ell} = r^{-1}[d(ru_\ell)/dr]$$

9

and the elements of the coefficient matrix $A_r(r)$ are no longer constant, but are functions of r. The corresponding equations for V and W are the same as equations (11) and (12) with y replaced by θ, the coefficient matrices being constant.

The systems of ordinary differential equations for the circumferential and axial displacements are solved in the same manner as equations (11) and (12), that is, by using an analogous solution to equation (14). For the case of equation (24) the solution is more complicated, since we no longer have constant coefficients. The solution may be expressed as (ref. 5).

$$U(r) = \Omega(A_r)U(r_0) + \Omega(A_r)\int_{r_0}^{r} [\Omega(A_r)]^{-1}R(\eta)d\eta \tag{26}$$

where r_0 is the initial value of r which may or may not be zero. The matrizant $\Omega(A_r)$ is given by the infinite matrix integral series

$$\Omega(A_r) = I + \int_{r_0}^{r} A_r(\eta_1)d\eta_1 + \int_{r_0}^{r} A_r(\eta_2)d\eta_2 \int_{r_0}^{\eta_2} A_r(\eta_1)d\eta_1$$

$$+ \int_{r_0}^{r} A_r(\eta_3)d\eta_3 + \int_{r_0}^{\eta_3} A_r(\eta_2)d\eta_2 \int_{r_0}^{\eta_2} A_r(\eta_1)d\eta_1 + \ldots \tag{27}$$

which of course becomes very difficult to evaluate. However, by substituting the matrix A_r into equation (27), it can be seen by inspection, (ref. 5), that $\Omega(A_r)$ can be partitioned into four submatrices which satisfy the following equations:

$$r^{-1}(d\Omega_{11}/dr) = \Omega_{21}$$

$$r(d\Omega_{21}/dr) = \Omega_{11}K_r$$

$$r^{-1}(d\Omega_{12}/dr) = \Omega_{22}$$

$$r(d\Omega_{22}/dr) = \Omega_{12}K_r \tag{28}$$

with

$$\Omega_{11}\big|_{r=r_0} = \Omega_{22}\big|_{r=r_0} = I$$

$$\Omega_{12}\big|_{r=r_0} = \Omega_{21}\big|_{r=r_0} = 0$$

and K_r is the submatrix of A_r obtained from the identity:

$$A_r = \begin{bmatrix} 0 & rI \\ r^{-1}K_r & 0 \end{bmatrix}$$

Instead of evaluating the matrizant $\Omega(A_r)$ by means of equation (27), it can be evaluated by solving equations (28). This was done for the examples presented herein, using a single step Runge-Kutta integration method for solving equations (28).

Since equations (10) to (12) and their boundary conditions are highly coupled, it is generally impossible to directly evaluate their solutions. Thus, a successive approximation procedure must be employed where assumed values must be used initially for the required unknowns. Once the displacement field in the body has been calculated and the successive approximation procedure has converged, the normal stress distributions can be obtained directly by using the stress-displacement relations. The shear stresses, however, can be evaluated only through finite difference approximations for the required displacement gradients.

All of the MOL work in three-dimensional fracture mechanics has been done using double precision arithmetic. With larger word sizes, 128 bits or greater, improved results can be obtained or more lines can be used. Typical problems on third generation computers can usually be handled with 100 to 200 lines in each direction using Cartesian coordinates, and up to 20 lines in each direction using cylindrical coordinates. Corresponding CPU times are of the order of 3 min for the elastic solution and 25 min for the entire elasto-plastic problem (ref. 6). Most of the computer time is spent in decoupling the three systems of simultaneous ordinary differential equations which arise in a general problem. Decoupling is done by a successive approximation procedure. With cyclic resubstitution of the obtained solutions into the coupling vectors and the boundary conditions good numerical convergence behavior was observed.

Elastic solutions have been obtained for typical fracture test specimen geometries such as the central crack, single edge crack, double edge crack and rectangular surface crack problems, all with uniform tensile loadings normal to the crack plane. In cylindrical coordinates, the problem of an embedded penny-shaped crack and the externally cracked circular cylinder in tension have been treated. Although shear and torsionally loaded specimens have not been analyzed previously by MOL, the necessary boundary conditions for these problems can be imposed without difficulties. Recently, the thumbnail crack problem was investigated in connection with applying MOL to curved crack boundaries (ref. 13). In addition, it seems that the common three-point bend specimen could also be analyzed in a systematic manner using this method.

Elasto-plastic solutions of certain crack problems have also been obtained using the incremental displacement formulation in connection with MOL (ref. 6). The nonlinear response of finite length cylinders with external annular cracks and a finite thickness rectangular plate containing a through-thickness central crack under uniaxial tension were studied in detail. In addition to the stresses and displacements, fracture mechanics parameters such

11

as the stress intensity factor, the J-integral and the load versus load point displacement plots were determined. Finally, the thumbnail crack problem was also studied, permitting small scale nonlinear material response.

STRESS INTENSITY AND STRAIN ENERGY DENSITY FACTORS

Since the application of boundary conditions for MOL allows the crack tip to remain between two successive node points, the exact location of crack tip together with the determination of K values for the elastic case is done by the first two terms in the Williams eigenfunction expansion. The crack face displacement and maximum normal stress near the crack front are used to find the coefficients in the two-term expansion. Assuming Cartesian coordinates and that y = 0 is the crack plane and that the crack is under normal tensile loading, we have

$$v = \alpha K_I \left[\sqrt{\frac{R + r}{2\pi}} + \frac{L_I}{K_I} \sqrt{(R + r)^3} \right] \tag{29}$$

$$\sigma_y = K_I \left[\frac{1}{\sqrt{2\pi(R - r)}} + \frac{L_I}{K_I} \sqrt{R + r} \right] \tag{30}$$

where α is a function of Poisson's ratio, the stress singularity is assumed to be $-1/2$, r is the crack edge position correction, v is the crack opening displacement, σ_y is the maximum normal stress and K_I and L_I are the mode I Williams expansion coefficients. Using displacement data from three adjacent nodes to the crack edge in equation (29), values of αK_I, L_I/K_I and r are calculated for each value of z, with R also measured from the half-way point between nodes specifying boundary stresses and displacements, respectively. Substituting values of L_I/K_I and r into equation (30), we can calculate K_I as a function of the corrected crack edge distance, $\rho = R - r$. Note that α would be equal to 3.56 for the plane strain case and 4.0 for the plane stress case with $\nu = 1/3$. Another approach to calculate K_I is to first determine the J_I integral and then use the linear elastic $J_I - K_I$ relation of the form (ref. 6)

$$K_I = \sqrt{\frac{E J_I}{1 - \nu^2}} \tag{31}$$

Linear fracture mechanics technology assumes then that the crack will propagate if K_I reaches its critical value K_{Ic}, usually called its fracture toughness. It should be noted that the K-concept is restricted to symmetric systems with the applied loads perpendicular to the crack plane and the crack propagating in a self-similar manner. In general, a complete description of the crack border stress field requires three stress intensity factors, and a mixed mode fracture criterion is needed to predict failure. To this end Sih (ref. 14) has defined a strain energy density factor, S, as

$$S = a_{11}k_1^2 + 2a_{12}k_1k_2 + a_{22}k_2^2 + a_{33}k_3^2 \tag{32}$$

12

where the coefficients $a_{ij}(i,j = 1,2)$ depend on the material constants and the angles θ and ω. Consistent with equation (32), the local stresses near the crack tip are of the form (ref. 14),

$$\sigma_x = \frac{k_1}{\sqrt{2\rho\cos\omega}} \cos\frac{\theta}{2}\left(1 - \sin\frac{\theta}{2}\sin\frac{3\theta}{2}\right)$$

$$- \frac{k_2}{\sqrt{2\rho\cos\omega}} \sin\frac{\theta}{2}\left(2 - \cos\frac{\theta}{2}\cos\frac{3\theta}{2}\right) + 0(1) \qquad (33)$$

Note that $k_i = K_i/\sqrt{\pi}$ and the coefficients a_{ij} are then given by equations of the form

$$16G \cos\omega\, a_{11} = (3 - 4\nu - \cos\theta)(1 + \cos\theta) \qquad (34)$$

As can be seen from equation (32), the stress intensity factors k_i still play an important role in the fracture process. Hence, the correct determination of these factors is a necessary step in the safe design of any structure. In the strain energy density failure criterion, it is assumed that the minimum value of S yields the direction of crack initiation and that the critical value of S_{min}, S_c, determines incipient fracture and is an intrinsic material property independent of the loading conditions and crack configurations.

Other multimode failure criteria have been proposed previously in the literature and a brief description of each fracture theory along with the limited experimental data can be found in (refs. 15 and 16). In general, little difference exists between theories predicting mode I, mode II interaction and combined damage crack propagation direction.

NUMERICAL RESULTS

A great amount of experimental work has been done in fracture mechanics using cracked specimens. Selected results for some common specimen geometries are shown in figures 3 to 16. Figure 3 shows a rectangular bar under normal tensile loading containing a traction free, through-thickness, central crack. The crack opening displacement at the middle and at the surface of the bar is plotted in figure 4, along with Raju's (ref. 17) finite element results. Stress intensity factor variations as a function of bar thickness are shown in figure 5. Variation of the constraint parameter β, defined as the quantity $\sigma_z/[\nu(\sigma_x + \sigma_y)]$, along the plate thickness is shown in figure 6. Note that for plane strain $\beta = 1$ and for plane stress case it vanishes. Figure 7 shows a bar with uniform tension containing a rectangular surface crack (ref. 18). Surface crack opening displacement as a function of crack depth is shown in figure 8 while the variation of the maximum normal stress σ_y is shown in figure 9 for a selected crack geometry. For the same rectangular surface crack problem, a plot of K_I along the crack periphery is shown in figure 10. The discretization of an externally cracked cylindrical fracture specimen is shown in figure 11. Crack face displacements for various crack lengths are plotted in figure 12 while the variation of K_I with crack length is shown in figure 13. Figure 14 is analogous to figure 11 but with an embedded, central, penny-shaped crack. The dimensionless crack opening displacements for various
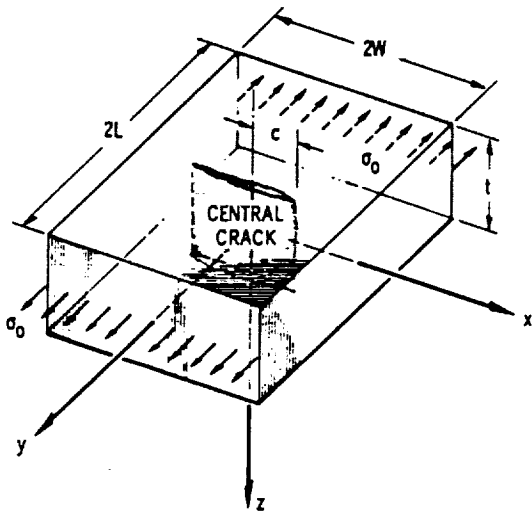
(a) RECTANGULAR BAR WITH THROUGH-THICKNESS CENTRAL
CRACK.
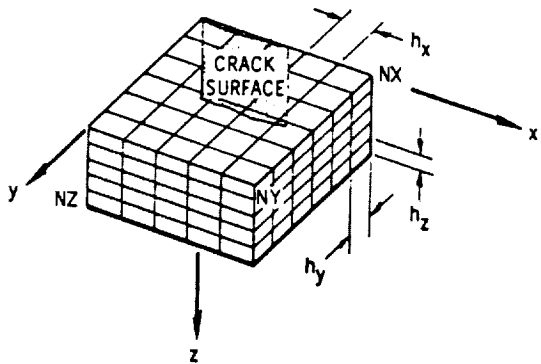
(b) DISCRETIZED REGION OF RECTANGULAR BAR WITH
THROUGH-THICKNESS CENTRAL CRACK.

FIGURE 3. - RECTANGULAR BAR WITH THROUGH-THICKNESS CENTRAL
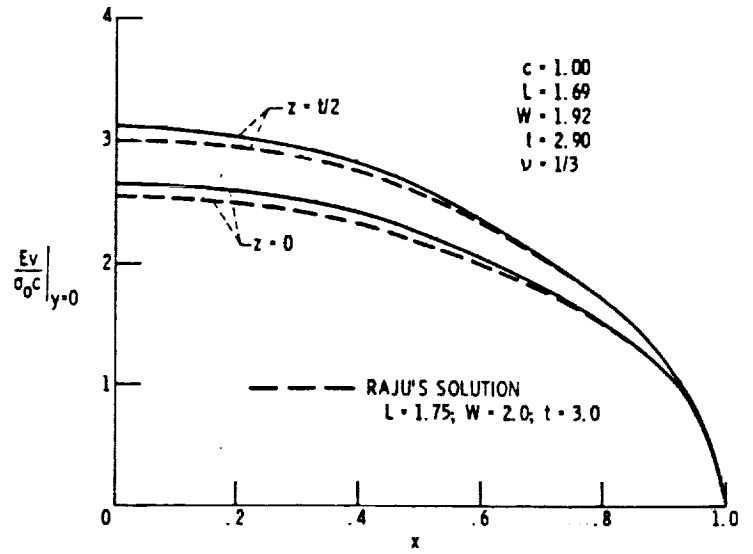CRACK UNDER UNIFORM TENSION.

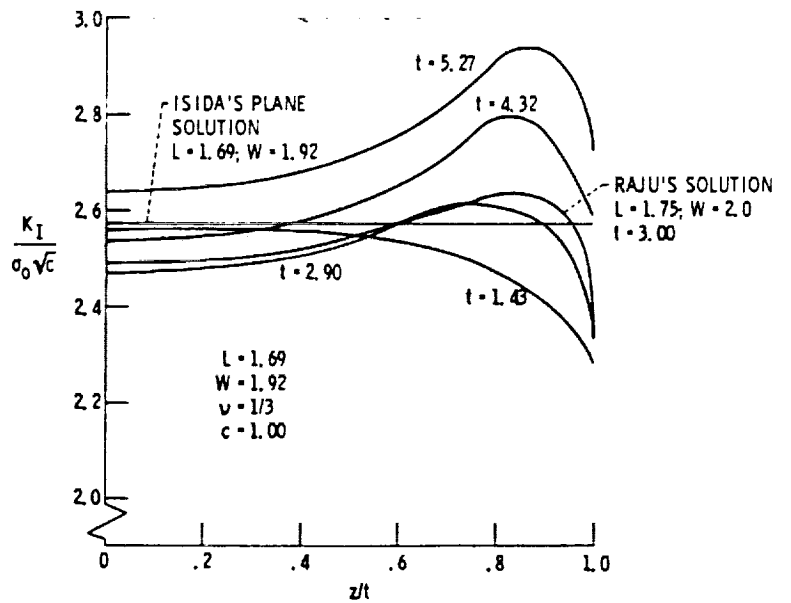FIGURE 4. - CRACK OPENING DISPLACEMENT FOR CENTER-CRACKED BAR
UNDER UNIFORM TENSION.

FIGURE 5. - STRESS-INTENSITY FACTOR VARIATION AS A
FUNCTION OF BAR THICKNESS FOR A CENTER-CRACKED REC-
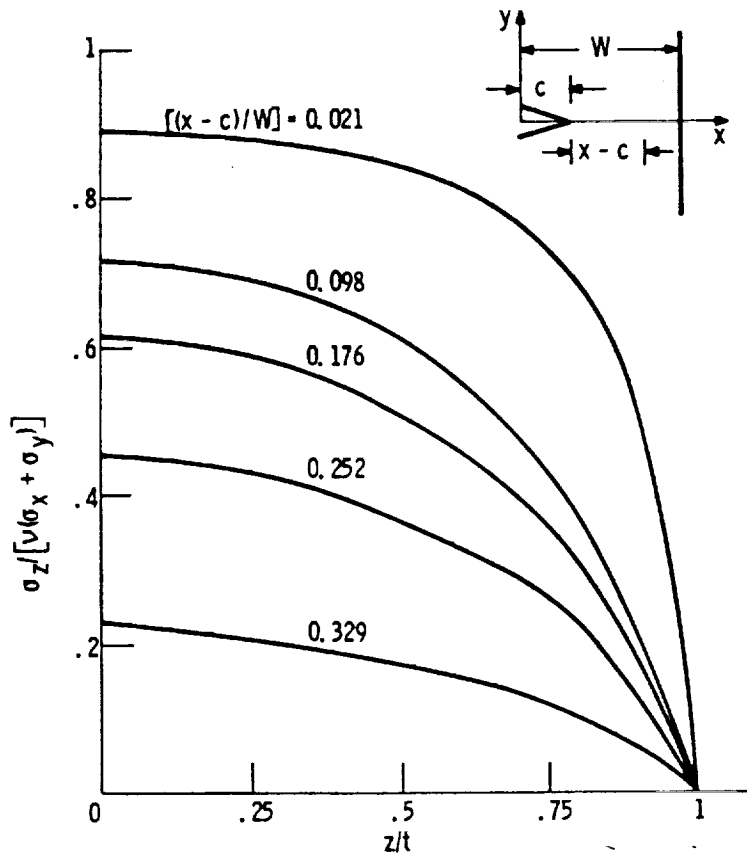TANGULAR BAR UNDER UNIFORM TENSION.

14

FIGURE 6. - VARIATION OF $\beta = \sigma_z/[\nu(\sigma_x + \sigma_y)]$ ON CRACK PLANE, y = 0. ACROSS PLATE THICKNESS. (c/W) = 0.5174. FOR IDEAL PLANE STRAIN CASE: $\beta = 1$, AND FOR PLANE STRESS: $\beta = 0$.

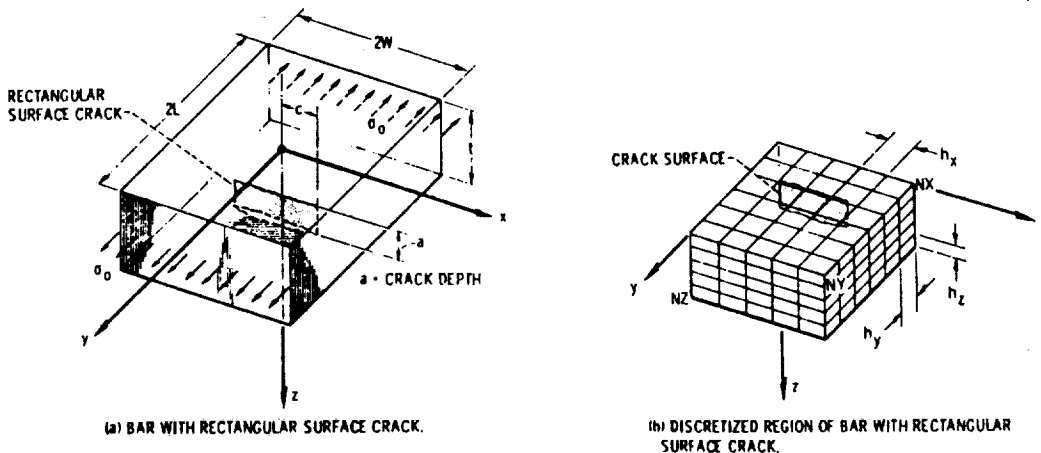(a) BAR WITH RECTANGULAR SURFACE CRACK.

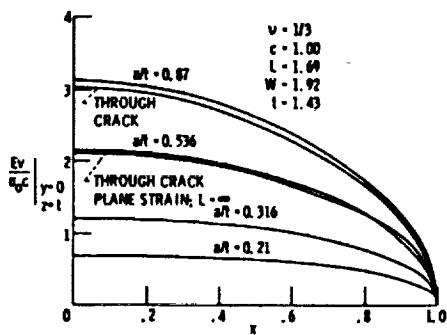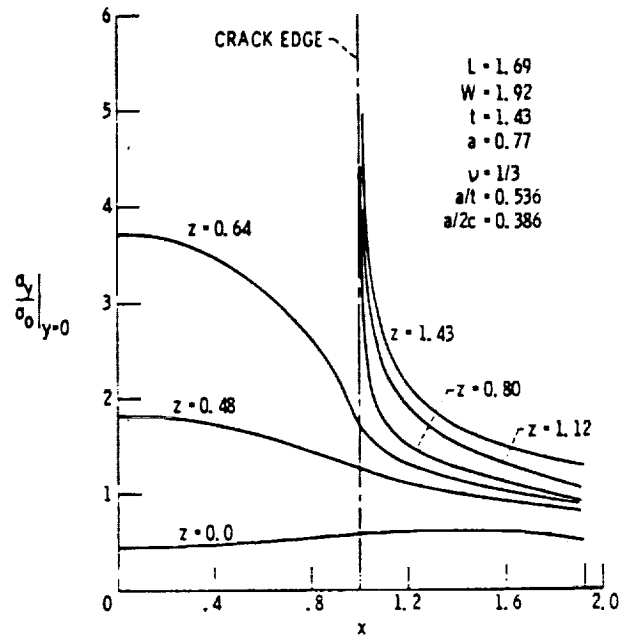(b) DISCRETIZED REGION OF BAR WITH RECTANGULAR SURFACE CRACK.

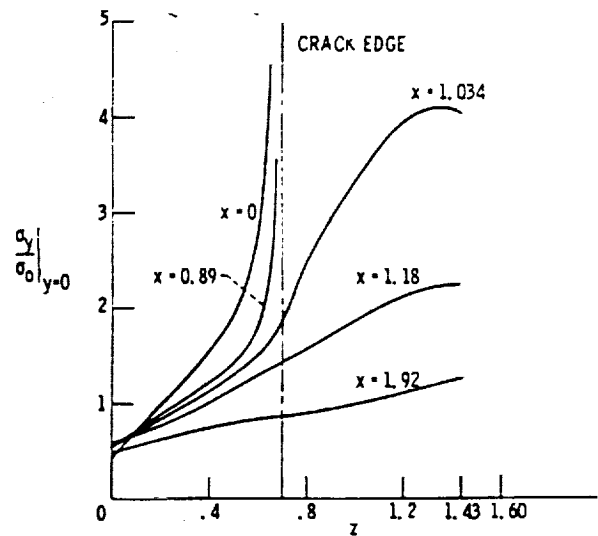FIGURE 7. - BAR WITH RECTANGULAR SURFACE CRACK UNDER UNIFORM TENSION.

15

FIGURE 8. – SURFACE CRACK OPENING DIS-
PLACEMENT VARIATION AS A FUNCTION OF
CRACK DEPTH FOR A RECTANGULAR BAR
UNDER UNIFORM TENSION.

(a) DIMENSIONLESS y-DIRECTIONAL NORMAL STRESS
VARIATION ALONG BAR WIDTH.

(b) DIMENSIONLESS y-DIRECTIONAL NORMAL STRESS
VARIATION ACROSS BAR THICKNESS.

FIGURE 9. – DIMENSIONLESS y-DIRECTIONAL NORMAL
STRESS DISTRIBUTION IN THE CRACK PLANE FOR A
BAR UNDER UNIFORM TENSION CONTAINING A RECTAN-
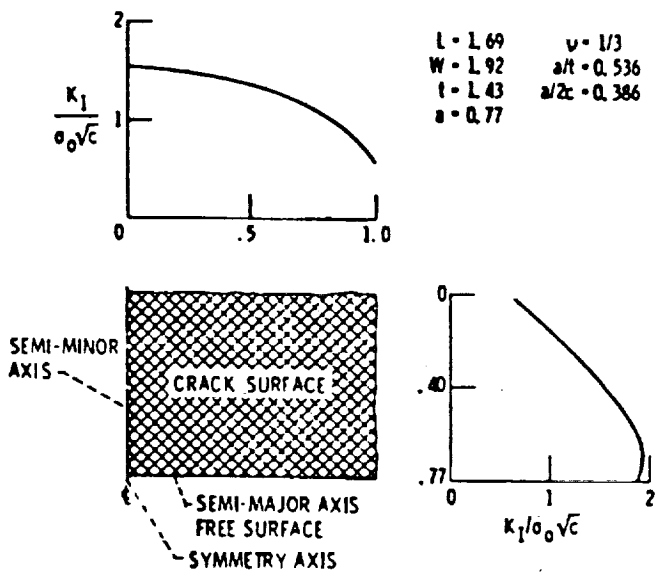GULAR SURFACE CRACK.

16

FIGURE 10. - VARIATION OF STRESS-INTENSITY FACTOR K_I ALONG THE CRACK PERIPHERY FOR A BAR UNDER TENSION CONTAINING A RECTANGULAR SURFACE CRACK.
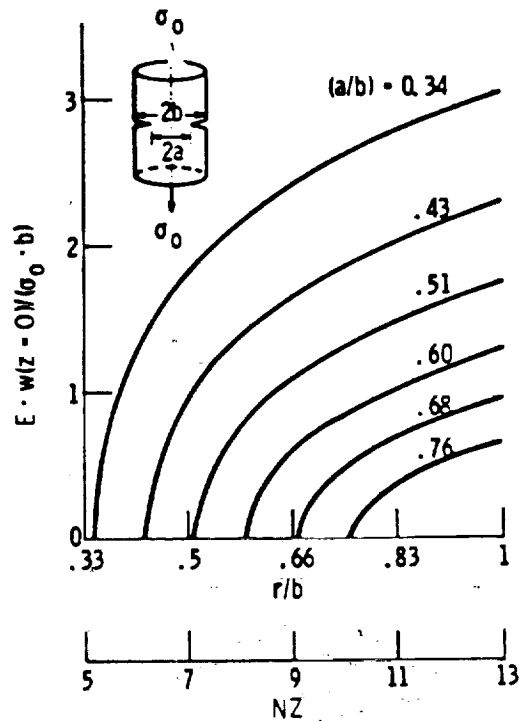
Within figure 10:

$L = 1.69$ $\nu = 1/3$
$W = 1.92$ $a/t = 0.536$
$t = 1.43$ $a/2c = 0.386$
$a = 0.77$

$\dfrac{K_I}{\sigma_0 \sqrt{c}}$

SEMI-MINOR AXIS
CRACK SURFACE
SEMI-MAJOR AXIS
FREE SURFACE
SYMMETRY AXIS

$K_I/\sigma_0 \sqrt{c}$

FIGURE 12. - CRACK FACE DISPLACEMENTS FOR VARIOUS CRACK LENGTHS.

Within figure 12:

$(a/b) = 0.34$
.43
.51
.60
.68
.76

$E \cdot w/(z - 0)/(\sigma_0 \cdot b)$

r/b

NZ
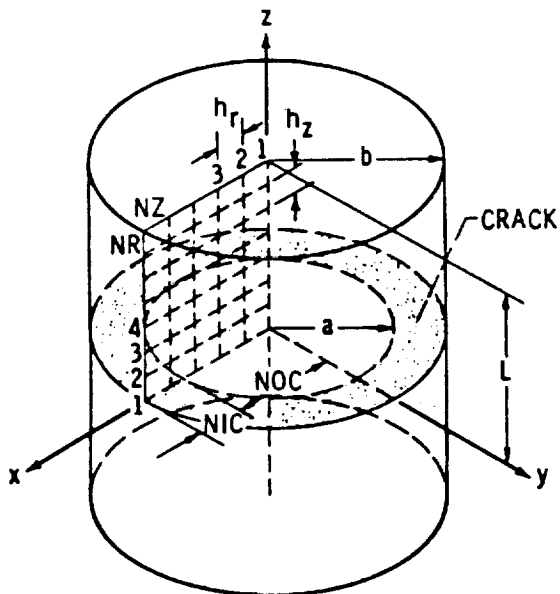

FIGURE 11. - DISCRETIZATION OF AN EXTERNALLY CRACKED CYLINDRICAL SPECIMEN.
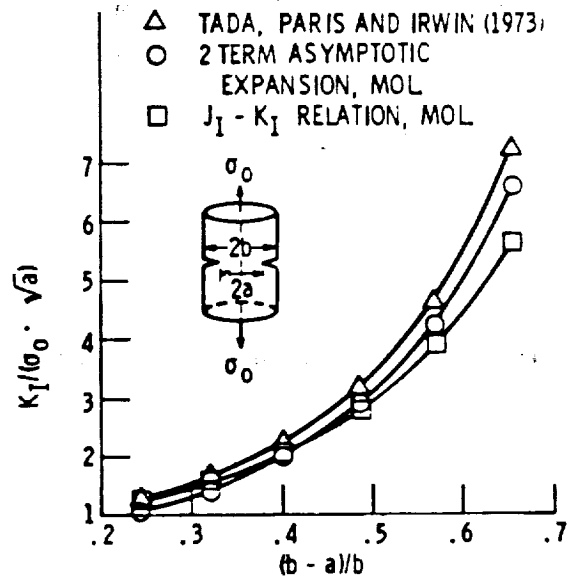
FIGURE 13. - VARIATION OF K_I WITH CRACK LENGTH.

Within figure 13:

△ TADA, PARIS AND IRWIN (1973)
○ 2 TERM ASYMPTOTIC EXPANSION, MOL
□ $J_I - K_I$ RELATION, MOL

$K_I/(\sigma_0 \cdot \sqrt{a})$

$(b - a)/b$
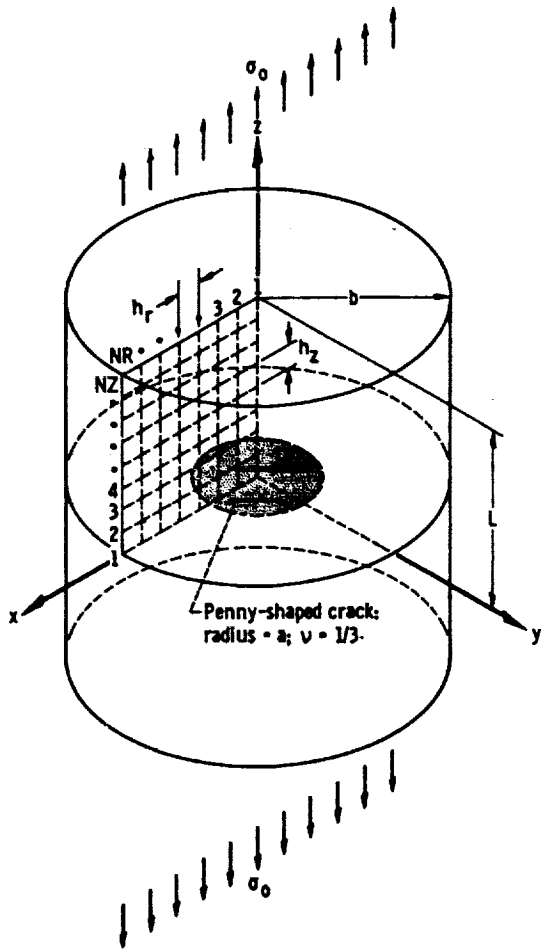
17

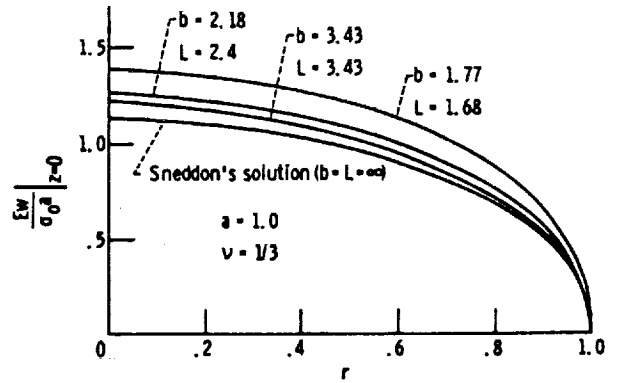FIGURE 14. - SOLID CYLINDRICAL BAR WITH PENNY-SHAPED CRACK.

FIGURE 15. - DIMENSIONLESS CRACK OPENING DISPLACE-MENTS FOR SOLID CYLINDRICAL BARS WITH PENNY-SHAPED CRACKS OF VARIOUS LENGTHS AND RADII.
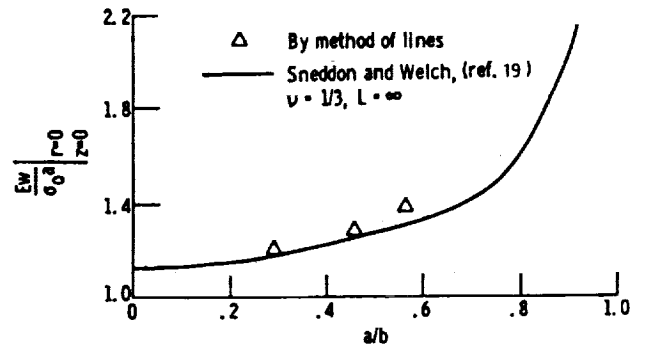

FIGURE 16. - DIMENSIONLESS MAXIMUM CRACK OPENING AS FUNCTION OF CRACK TO CYLINDER RADIUS RATIO.

geometry cylinders are plotted in figures 15 and 16 and are compared to Sneddon's (ref. 19) closed form solution. It is obvious from these results that a variety of plots familiar to the fracture mechanics community can be constructed, since MOL methods give complete field solutions.

CONCLUDING REMARKS

The line method of analysis is a practical approach for the solution of three-dimensional crack problems, at least for bodies with reasonably regular boundaries. Both elastic and inelastic solutions can be obtained. Just how efficient the method is or can be made is not fully established. It is known, however, that good results are obtained from the use of relatively coarse grids. Interestingly, displacements and normal stresses are determined with equal accuracy since numerical differentiation of the displacements is not required. Applications to curved boundaries, bending or shear modes of loading and variable mesh spacing are some of the current areas that need additional investigations. Furthermore, improvements in computer hardware, such as the use of super computers, could help overcome some of the presently experienced stability problems.

REFERENCES

1. Gallagher, R.H.: A Review of Finite Element Techniques in Fracture Mechanics. Numerical Methods in Fracture Mechanics, A.R. Luxmoore and D.R.J. Owen, eds., University College Swansea, 1978, pp. 1-25.

2. Levy, N.; and Marcal, P.V.: Three-Dimensional Elastic-Plastic Stress and Strain Analysis for Fracture Mechanics, Phase I: Simple Flawed Specimens; Phase II: Advanced Flawed Specimens. USAEC Report HSSTP-TR-12, 1970.

3. Ayres, D.J.: A Numerical Procedure for Calculating Stress and Deformation Near a Slit in a Three-Dimensional Elastic-Plastic Solid. NASA TM X-52440, 1968.

4. Cruse, T.A.; and Wilson, R.B.: Boundary Integral Equation Method for Elastic Fracture Mechanics Analysis. Air Force Office of Scientific Research, AFOSR-TR-78-0355, 1978. (Avail. NTIS, AD-A051992).

5. Gyekenyesi, J.P.; and Mendelson, A.: Three-Dimensional Elastic Stress and Displacement Analysis of Finite Geometry Solids Containing Cracks. Int. J. Fract., vol. 11, no. 2, 1975, pp. 409-429.

6. Malik, S.N.: Elasto-Plastic Analysis for Finite Geometry Cracked Members by the Method of Lines. Ph. D. Dissertation, Ohio State University, 1979.

7. Liskovets, O.A.: The Method of Lines (Review). Diff. Equations, vol. 1, 1965, pp. 1308-1323.

8. Jones, D.J.; South, J.C. Jr.; and Klunker, E.B.: On the Numerical Solution of Elliptic Partial Differential Equations by the Method of Lines. J. Comput. Phys., vol. 9, June 1972, pp. 496-527.

9. Irobe, M.: Method of Numerical Analysis for Three-Dimensional Elastic Problems. 16th Jpn National Congress of Applied Mechanics Proceedings, Central Scientific Publ., 1968, pp. 1-7.

10. Faddeva, V.N.: The Method of Lines Applied to Some Boundary Problems. Trudy Mat. Inst. Steklov., vol. 28, 1949, pp. 73-103. (In Russian).

11. Loeb, A.M.; and Schiesser, W.E.: Stiffness and Accuracy in the Method of Lines Integration of Partial Differential Equations. Stiff Differential Systems, R.A. Willoughby, ed., Plenum Press, 1974, pp. 229-243.

12. Janac, K.: Adaptive CSDT Algorithms for Multidimensional Equations. Advances in Computer Methods for Partial Differential Equations - II, R. Vichnevetsky, ed., IMACS, 1977, pp. 214-220.

13. Mendelson, A.; and Alam, J.: Solution of Elastic and Elasto-Plastic Problems by the Method of Lines. NASA CR-168125, 1983.

14. Sih, G.C.: Mechanics of Fracture: Linear Response. Numerical Methods in Fracture Mechanics, A.R. Luxmoore and D.R.J. Owen, eds., University College Swansea, 1978, pp. 155-192.

15. Feldman, A.; Smith, F.W.; and Holston, A., Jr.: Characterization of Crack Growth Under Combined Loading. NASA CR-135197, 1977.

16. Shah, R.C.: Effects of Proof Loads and Combined Mode Loadings on Fracture and Flaw Growth Characteristics of Aerospace Alloys. NASA CR-134611, 1974.

17. Raju, I.S.; and Newman, J.C., Jr.: Three-Dimensional Finite Element Analysis of Finite Thickness Fracture Specimens. NASA TN D-8414, 1977.

18. Gyekenyesi, J.P.; and Mendelson, A.: Stress Analysis and Stress Intensity Factors for Finite Geometry Solids Containing Rectangular Surface Cracks. J. Appl. Mech., vol. 44, no. 3, Sept. 1977, pp. 442-448.

19. Sneedon, I.N.; and Welch, J.T.: A Note on the Distribution of Stress in a Cylinder Containing a Penny-Shaped Crack. Int. J. Eng. Sci., vol. 1, no. 3, 1963, pp. 411-419.

1. Report No. NASA TM–103626	2. Government Accession No.	3. Recipient's Catalog No.
4. Title and Subtitle The Method of Lines in Analyzing Solids Containing Cracks		5. Report Date November 1990
		6. Performing Organization Code
7. Author(s) John P. Gyekenyesi		8. Performing Organization Report No. E–5794
		10. Work Unit No. 505–63–5B
9. Performing Organization Name and Address National Aeronautics and Space Administration Lewis Research Center Cleveland, Ohio 44135–3191		11. Contract or Grant No.
		13. Type of Report and Period Covered Technical Memorandum
12. Sponsoring Agency Name and Address National Aeronautics and Space Administration Washington, D.C. 20546–0001		14. Sponsoring Agency Code

15. Supplementary Notes

16. Abstract

A semi-numerical method is reviewed for solving a set of coupled partial differential equations subject to mixed and possibly coupled boundary conditions. The line method of analysis is applied to the Navier-Cauchy equations of elastic and elastoplastic equilibrium to calculate the displacement distributions in various, simple geometry bodies containing cracks. The application of this method to the appropriate field equations leads to coupled sets of simultaneous ordinary differential equations whose solutions are obtained along sets of lines in a discretized region. When decoupling of the equations and their boundary conditions is not possible, the use of a successive approximation procedure permits the analytical solution of the resulting ordinary differential equations. The use of this method is illustrated by reviewing and presenting selected solutions of mixed boundary value problems in three-dimensional fracture mechanics. These solutions are of great importance in fracture toughness testing, where accurate stress and displacement distributions are required for the calculation of certain fracture parameters. Computations obtained for typical flawed specimens include that for elastic as well as elastoplastic response. Problems in both Cartesian and cylindrical coordinate systems are included. Results are summarized for a finite geometry rectangular bar with a central through-the-thickness or rectangular surface crack under remote uniaxial tension. In addition, stress and displacement distributions are reviewed for finite circular bars with embedded penny-shaped cracks, and rods with external annular or ring cracks under opening mode tension. The results obtained show that the method of lines presents a systematic approach to the solution of some three-dimensional mechanics problems with arbitrary boundary conditions. The advantage of this method over other numerical solutions is that good results are obtained even from the use of a relatively coarse grid.

17. Key Words (Suggested by Author(s)) Navier-Cauchy equations; Method of lines; Displacements; Stresses; Cracks; Stress intensity factors; Finite differences; Stability; Successive approximations; Cartesian, cylindrical coordinates; Differential equations	18. Distribution Statement Unclassified – Unlimited Subject Category 39

19. Security Classif. (of this report) Unclassified	20. Security Classif. (of this page) Unclassified	21. No. of pages	22. Price*